Direct measurements of impurity and lattice components of the nuclear spin-lattice relaxation in Al_2O_3 crystals

Direct measurements of impurity and lattice components of the nuclear spin–lattice relaxation in Al$_2$O$_3$ crystals

E V Charnaya†, V M Mikushev and E S Shabanova

Institute of Physics, St-Petersburg State University, St Petersburg, 198904, Russia

Abstract. For ^{27}Al nuclei in Al$_2$O$_3$ crystals, both nominally pure and doped with Cr^{3+}, suppression of the impurity nuclear spin–lattice relaxation under the condition of additional stationary magnetic saturation of the NMR line has been observed for the first time. Measurements of the lattice and impurity components of the spin–lattice relaxation time have been performed. The study was carried out at 77 K for different crystal orientations. Possible mechanisms of the impurity NMR relaxation suppression are discussed.

1. Introduction

The nuclear spin–lattice relaxation time T_1 is one of the most significant parameters in radio-frequency spectroscopy. In real crystals this time is known to be determined by contributions from two components: a lattice component providing relaxation in an ideal sample and an impurity component. In this connection the total relaxation process is characterized by the time [1, 2]

$$\left(T_1^{\Sigma}\right)^{-1} = \left(T_1^{\text{lat}}\right)^{-1} + \left(T_1^{\text{imp}}\right)^{-1} \tag{1}$$

where T_1^{lat} is the lattice component and T_1^{imp} is due to impurities. The magnitude of T_1^{imp} gives an idea of the impurity content of the materials of interest, whereas the time T_1^{lat} gives information on the crystal structure. Until recently it has not been possible to measure T_1^{lat} and T_1^{imp} separately in a given sample. The impurity component has been identified either by invoking model-based arguments [1–5] regarding the time, the temperature or the field dependences of the restoration of the magnetization signal or by making a comparison with samples regarded as defect free. These two methods can give only estimates and leave uncertainties in the contributions of T_1^{lat} and T_1^{imp}.

In [6–9] a fundamentally new method of separating and directly measuring the lattice and impurity contributions to the total relaxation time has been suggested. That method is based on the use of a version of double nuclear resonance: the saturation of the signal of the nuclear free precession after a $\pi/2$ pulse by additional electric, acoustic or magnetic steady-state resonance fields. The principle is as follows.

The impurity spin–lattice relaxation takes place owing to the more rapid relaxation processes in the vicinity of the paramagnetic centres than in a perfect lattice [1, 2, 5]. As a result, the local inverse spin temperature α_{loc} in the defect region, which is proportional to

† Temporary address: Department of Physics, Cheng Kung State University, Tainan, Taiwan.

the local nuclear magnetization, is closer to the equilibrium inverse lattice temperature α_1, than the average value $\langle \alpha \rangle$ in the volume:

$$|\alpha_{loc} - \alpha_1| < |\langle \alpha \rangle - \alpha_1|. \tag{2}$$

A local spin temperature change spreads through the sample volume by means of spin diffusion. Inequality (2) is the condition for effective impurity spin–lattice relaxation. Most methods for measuring the spin–lattice relaxation time are based on the magnetization signal recovery occurring after a $\pi/2$ pulse, i.e. after the pulse saturation corresponding to $\langle \alpha \rangle = 0$. For these methods the impurity spin–lattice relaxation proceeds under the condition $\alpha_{loc} > \langle \alpha \rangle$ following from the inequality (2). The last condition means that for a positive spin temperature the impurity relaxation occurs when the spin system in an impurity region is colder than on average over the crystal. If the region near the impurity is saturated by additional resonance fields up to $\alpha_{loc} = 0$, then this region becomes hotter. In that case, spin diffusion should promote heating of the nuclear spin system via impurities. This effect is similar to dynamic nuclear polarization by fixed paramagnetic centres [1,5,10]. Thus, under local saturation, the impurity relaxation becomes suppressed and restoration of the average magnetization over the volume will be determined exclusively by the lattice mechanism. This gives us the possibility of obtaining the time T_1^{lat} and of calculating T_1^{imp} by equation (1).

It has been shown in [11–13] that effective local heating of the nuclear spin system can arise under conditions of acoustic or electric saturation of the NMR line because the induced transition probabilities, as well as the ratios of the induced transition probability to the relaxation transition probability, are considerably greater near paramagnetic impurities than in the regular lattice. Using these results, the separation of relaxation times has been demonstrated in [6,7] for Ga^{69} and Ga^{71} in nominally pure and doped high-resistivity GaAs crystals under the electric saturation condition. Similarly, direct measurement of T_1^Σ, T_1^{lat} and T_1^{imp} has been performed for the case of acoustic and magnetic additional resonance steady-state fields for Na^{23} in NaI and NaCl crystals in [7–9].

The effect of the suppression of impurity relaxation can be tested in another way, by measuring the spin relaxation time after a π pulse which reverses the nuclear magnetization [8]. In the first step of restoration of magnetization $\langle \alpha \rangle$ is negative and the inequality (2) holds independently of the local spin-system saturation. Hence, the restoration of nuclear magnetization should be determined by the quantity of T_1^Σ, while above $\langle \alpha \rangle = 0$ the magnetization recovery process should be the same as in the case of a $\pi/2$ pulse. The results obtained for NaI crystals [8] have confirmed these suggestions.

The experimental results [6–9] cited above have been obtained for cubic crystals. The separation of the lattice and impurity relaxations under stationary nuclear spin-system saturation has not previously been studied in non-cubic crystals.

In the present paper we report the separation of lattice and impurity relaxations for ^{27}Al in hexagonal Al_2O_3 crystals under the condition of magnetic stationary saturation.

2. Samples and experimental procedure

The studies were carried out for two Al_2O_3 samples: colourless nominally pure material (sapphire) and light-pink material doped with Cr^{3+} ions to the concentration of 0.03 at.% (ruby). Each sample was a cylinder with the axis perpendicular to the crystal C axis. The measurements of the ^{27}Al ($I = \frac{5}{2}$) nuclear free-precession signal were performed at 77 K at a constant magnetic field strength $B_0 = 0.5$ T for the orientations $\Theta = 0°$, $90°$ and $54°$ (magic angle Θ_m), where Θ is the angle between the crystal C axis and the magnetic field.

The stationary saturation of the nuclear-free-precession signal was performed by applying an additional magnetic field at the resonance frequency by means of the additional coil. The saturation level was characterized by the saturation factor Z which is given [10] by

$$Z = \langle \alpha \rangle_{st}/\alpha_l \qquad (3)$$

where $\langle \alpha \rangle_{st}$ is the value of $\langle \alpha \rangle$ for stationary saturation. The factor Z was measured as the ratio of the free-precession signal amplitudes after a $\pi/2$ pulse with the additional magnetic field switched on and off.

It should be noted that under saturation conditions the magnetization is restored within a time τ which differs from the spin–lattice relaxation time T_1. The times τ and T_1 are related to one another by [6]

$$\tau = ZT_1. \qquad (4)$$

To find the time τ of the magnetization recovery due to the spin–lattice relaxation, the nuclear free-precession signal amplitude A was measured as a function of a time t after the pulse saturation. It is well known that the nuclear magnetization recovery for nuclei with spin $I > \frac{1}{2}$ in non-cubic crystals is a complicated process [1] because the energy levels are shifted by the quadrupole interaction. For Al$_2$O$_3$ crystals the peculiarities in the ^{27}Al NMR spectrum and spin–lattice relaxation characteristics in the absence of saturation have been studied in detail in [14–16]. It has been shown, in particular, that the model of impurity relaxation accompanied by the spin diffusion [1,5] gives the most adequate description of the relaxation process in ruby. According to this model the magnetization recovery, when the crystal is oriented at the magic angle and the energy levels are nearly equidistant, follows an exponential law with a single relaxation time T_1^Σ given by equation (1). Hence, for the orientation at a magic angle we can calculate the time τ as usual from the slope of a graph of $-\ln[1 - A(t)/A_0]$ versus t, where A_0 is the equilibrium amplitude under stationary saturation.

However, at $\Theta = 0°$ or $90°$, when the energy levels are not equidistant, the total relaxation process is the superposition of several exponential processes [15] and the plot of $-\ln[1 - A(t)/A_0]$ versus t is no longer a straight line. Also, the time characteristics of relaxation are different for different pairs of spin levels. To study the suppression of impurity relaxation at these angles we excited transitions between levels with $m = \pm\frac{1}{2}$, where m was the magnetic quantum number. In this case the magnetization recovers as a sum of three exponentials [15]. To characterize the recovery process we used an average time $\langle \tau \rangle$ defined by

$$\langle \tau \rangle = -\Delta t / \ln\left[1 - A(\Delta t)/A_0\right]. \qquad (5)$$

In (5) the interval Δt after the pulse saturation was taken to be equal to $5\tau_{max}$, where τ_{max} was the longest of three times describing the magnetization recovery. It was calculated from the slope of linear part of the plot of $-\ln[1 - A(t)/A_0]$ versus t at long t [15].

3. Experimental results

The experimental dependence of the recovery time τ as a function of the factor Z in nominally pure Al$_2$O$_3$ for the orientation Θ_m is shown in figure 1. In figure 2 there are shown, as as example, two curves of $-\ln[1 - A(t)/A_0]$ versus t from which the times τ have been calculated. Without the additional stationary saturation the saturation factor

and the recovery time are $Z = 1$ and $\tau = T_1^{\Sigma}$, respectively. In the Z-range from 1.0 to 0.7 the dependence $\tau(Z)$ is linear which gives for T_1^{Σ} the value of 110 ± 5 s. In the range $0.4 < Z < 0.7$ a departure of the $\tau(Z)$-dependence from linearity is observed; this is due to incomplete suppression of the impurity relaxation. For $Z < 0.4$ the dependence $\tau(Z)$ becomes linear again, which corresponds to full suppression of the impurity spin–lattice relaxation channel. In this case the relaxation is caused only by the lattice mechanism and is characterized by the time T_1^{lat}. One can estimate this time from the $\tau(Z)$ slope at $Z < 0.4$, which gives $T_1^{lat} = 270\pm30$ s. From equation (1) we obtain $T_1^{imp} = 180\pm20$ s. Thus, the impurity relaxation even in the nominally pure Al_2O_3 sample is a substantial contribution to the spin–lattice relaxation process. This contribution can be attributed to the influence of a small number of impurities.
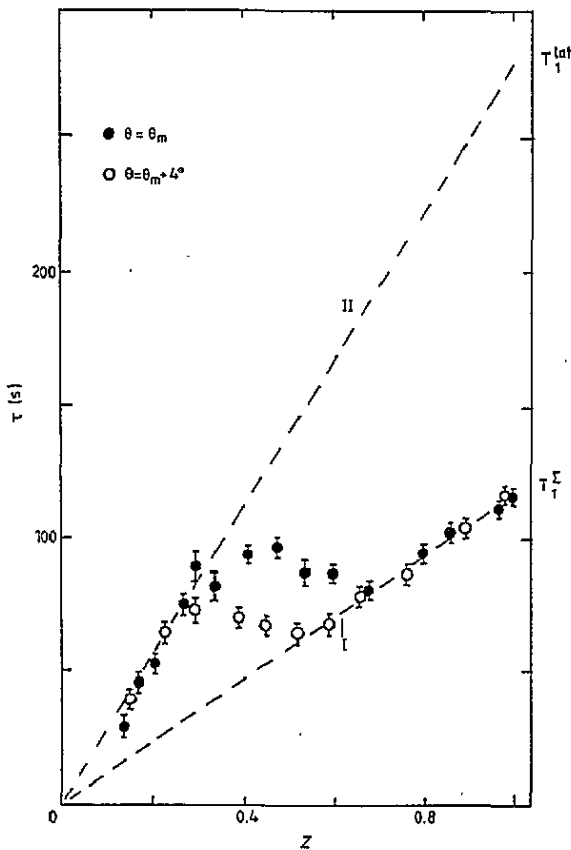

Figure 1. The restoration time τ versus saturation factor Z in sapphire at $\Theta = \Theta_m$ and $\Theta = \Theta_m + 4°$. - - - -, *dependences $\tau(Z)$ without impurity relaxation suppression (line I) and for lattice mechanism only (line II).*

The dependence $\tau(Z)$ for the orientation $\Theta = \Theta_m + 4°$ is also represented in figure 1. Such a small variation in orientation does not significantly change the system of NMR levels; nonetheless, the impurity channel suppression occurs at $Z = 0.5$–0.3, which is less than in the previous case. These results demonstrate a strong dependence of the impurity channel suppression efficiency on the crystal orientation.

The plot of τ versus Z for the light-pink ruby for $\Theta = \Theta_m$ is shown in figure 3. It gives $T_1^{\Sigma} = 5.0\pm0.2$ s. The value of T_1^{Σ}, smaller than that for nominally pure Al_2O_3, is associated with the Cr^{3+} impurities. The lattice contribution does not depend on the impurity concentration; we can estimate $T_1^{imp} = 5.1\pm0.6$ s for the ruby under study. In
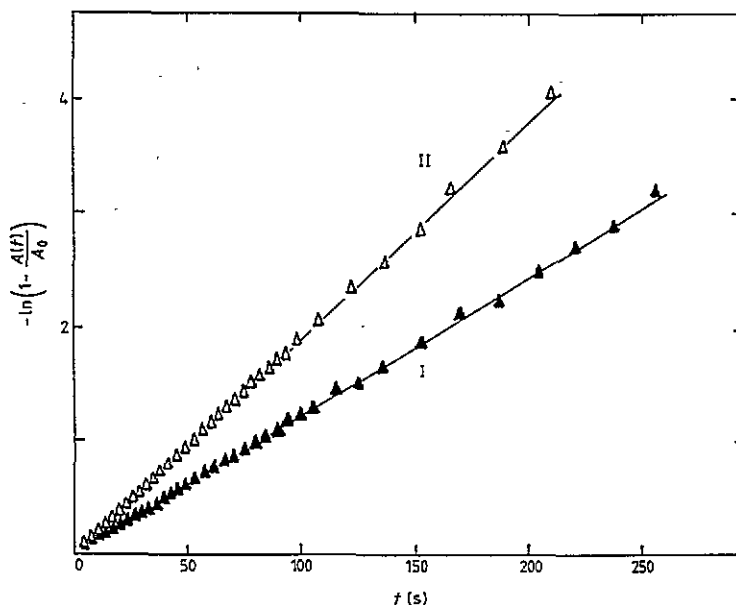
Figure 2. The plot of $-\ln[1 - A(t)/A_0]$ versus t for sapphire at $\Theta = \Theta_m$ under steady-state saturation with $Z = 0.8$ (line I) and $Z = 2.0$ (line II).
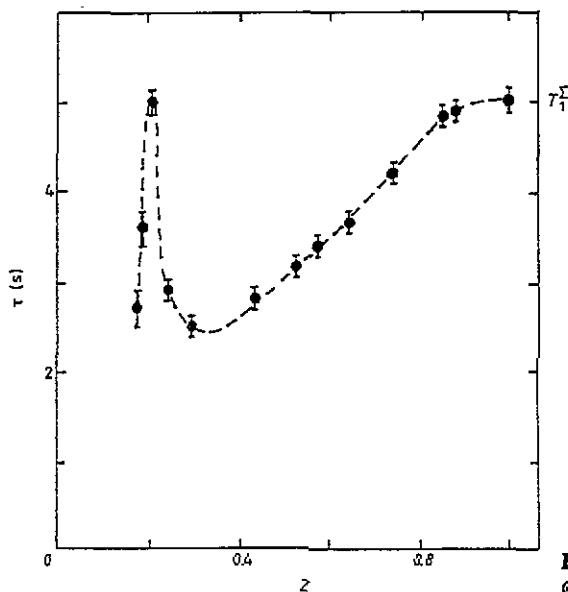

Figure 3. The dependence $\tau(Z)$ for ruby at $\Theta = \Theta_m$: - - - -, guide for eye.

the Z-range of 0.15–0.20 the experimental curve cannot be approximated by a straight line passing through the origin. This behaviour can be explained by the incomplete suppression of impurity relaxation for a high concentration of paramagnetic Cr^{3+} ions, probably because of the formation of impurity complexes.

The determination of spin–lattice relaxation times for the system of non-equidistant levels ($\Theta = 0°$ and 90°) is difficult because the spin–lattice relaxation is not described by a single exponent [15]. This introduces uncertainties into the estimation of the restoration

time. The experimental results for the average restoration time $\langle \tau \rangle$ for pure Al_2O_3 and ruby for the case of the non-equidistant ^{27}Al level system are shown in figure 4 and figure 5. For both samples the dependences of $\langle \tau \rangle(Z)$ reveal the impurity relaxation suppression at a saturation level which depends on the impurity concentration and on the crystal orientation. The different slopes of the initial parts of the $\langle \tau \rangle(Z)$ curves for pure Al_2O_3 and ruby can be caused by incomplete impurity relaxation suppression for ruby as in the case of Θ_m.
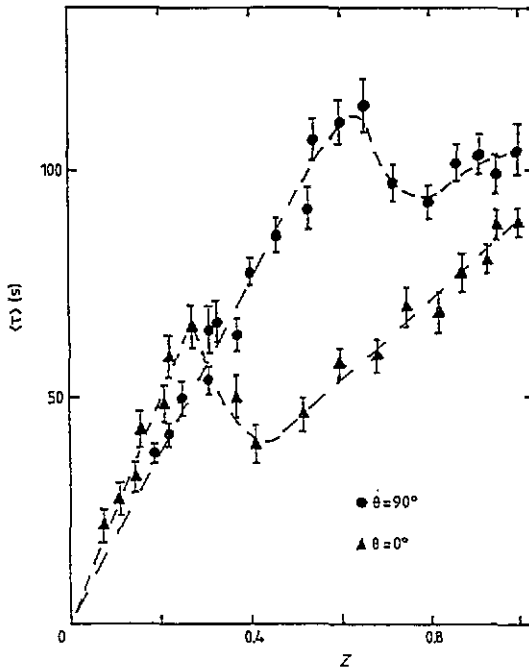

Figure 4. The plot $\langle \tau \rangle$ versus Z for sapphire at $\Theta = 0$ and 90°: dashed, guides for eye.

It should be noted that the curves showing the impurity relaxation suppression, similar to that in figures 4 and 5, can be plotted also for τ_{max} or for any other restoration time, calculated from different parts of the graph of $-\ln[1 - A(t)/A_0]$ versus t. Thus, one can conclude that the model of impurity relaxation suppression remains valid for a non-equidistant nuclear spin levels.

Our experimental data on the times T_1^{Σ}, T_1^{lat} and T_1^{imp} are listed in table 1. Since the time T_1^{lat} is a lattice structure characteristic and is independent of the impurity concentration, we assumed the time T_1^{lat} in ruby to be the same as in pure Al_2O_3 at the same orientation.

Table 1. Experimental data on T_1^{Σ}, T_1^{lat} and T_1^{imp}.

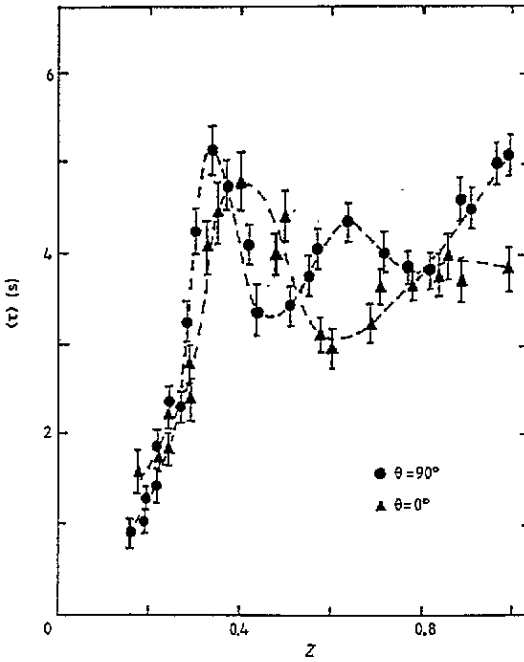| Sample	Θ (deg)	T_1^{Σ} (s)	T_1^{lat} (s)	T_1^{imp} (s)
Pure Al_2O_3	Θ_m	110±5	270±30	180±20
Pure Al_2O_3	0	90±5	250±40	140±20
Pure Al_2O_3	90	105±6	140±30	240±40
Ruby	Θ_m	5.0±0.2	—	5.1±0.6
Ruby	0	3.8±0.5	—	3.9±0.9
Ruby	90	5.2±0.6	—	5.3±0.9

Figure 5. The plot $\langle \tau \rangle$ versus Z for ruby at $\Theta = 0$ and 90°: dashed, guides for eye.

4. Theoretical models

The experimentally obtained value of T_1^{imp} in ruby can be compared with the theoretically estimated value, which is given by the theory of the impurity relaxation accompanied by the spin diffusion (the model of non-interacting impurities) [1, 2, 5]:

$$\left(T_1^{imp}\right)^{-1} = 8.5 \, NC^{1/4}D^{3/4} \tag{6}$$

where N is the impurity concentration, C is the inverse time of the nuclear relaxation due to the impurity at the unit distance from this impurity, and D is the spin diffusion coefficient. Using theoretical calculations of C- and D-values for ruby from [15], $C = 0.7 \times 10^{-42}$ cm^6 s^{-1}, $D = 4.2 \times 10^{-13}$ cm^2 s^{-1}, and the impurity concentration N for the ruby under study is 1.4×10^{18} cm^{-3}, the time $T_1^{imp} = 1.6$ s has been obtained, which is in good accordance with our experimental value equal to 5.1 ± 0.6 s.

Let us consider possible impurity NMR relaxation suppression mechanisms for the case of additional stationary magnetic saturation. Impurity relaxation suppression takes place when

$$W_{loc}T_1^{loc} > WT_1^{\Sigma} \tag{7}$$

where W_{loc} is the probability of induced nuclear spin transitions near defects, W is the probability of the nuclear spin transitions due to the interaction with the saturation field in the ideal crystal and T_1^{loc} is the nuclear spin–lattice relaxation time in the vicinity of the defects. One can estimate the time T_1^{loc} taking into account that $C^{-1} = T_1^{loc}(r)r^{-6}$, where r is the distance between the paramagnetic ion and the nucleus [1, 5]. It is possible to calculate the probability W_{loc} if we assumed that induced nuclear spin transitions in the impurity vicinity are due to the indirect interaction with the saturation magnetic field. This interaction involves the coupling of the paramagnetic centre with the saturation field and the magnetic interaction of the centre with neighbouring nuclei. The smallest value of the

interaction of the centre with neighbouring nuclei can be obtained if we take into account only a dipole–dipole component which depends on the distance as r^{-3}. Also, the main contribution comes from the part of interactions involving z-projection of the electron spin operator. Using the above-mentioned values [15] of C and T_1^{Σ}, and expressions for W and for the Cr^{3+} ion interaction with the magnetic field and neighbouring nuclei [17], it is not difficult to show (in Gaussian units) that

$$\frac{W_{loc}T_1^{loc}}{WT_1^{\Sigma}} = \frac{1.4 \times 10^{42}g^4\beta^4}{\hbar^2\gamma^2 B_0^2} \simeq 100 \tag{8}$$

where B_0 is the constant magnetic field, g is the electronic g-factor, β is the Bohr magneton and γ is the nucleus gyromagnetic ratio. Estimate (8) is in accordance with the condition (7).

It should be noted that the value of W_{loc}/W has been underestimated because we have included only the dipole–dipole contribution in an interaction with neighbouring nuclei.

Unfortunately, it is not possible to obtain analogous estimates for the nominally pure crystal under study because the impurities are unknown.

In conclusion, the present study reveals a new possibility for impurity channel suppression of the nuclear spin–lattice relaxation in non-cubic crystals under the additional magnetic saturation in the particular case of Al_2O_3 crystals. The time T_1^{lat} which is the characteristic of the Al_2O_3 lattice has been obtained.

Acknowledgment

References

[1]   Abragam A 1989 *Principles of Nuclear Magnetism* (Oxford: Clarendon)
[2]   Abragam A and Goldman M 1982 *Nuclear Magnetism: Order and Disorder* (Oxford: Oxford University Press)
[3]   Waugth J S and Slichter C P 1988 *Phys. Rev.* B **37** 4337
[4]   Waugth J S and Slichter C P 1989 *Phys. Rev.* B **40** 4203
[5]   Khutsishvili G R 1965 *Sov. Phys.–Usp.* **8** 743
[6]   Efitsenko P Yu, Mikushev V M and Charnaya E V 1991 *JETP Lett.* **54** 587
[7]   Efitsenko P Yu, Mavlonazarov I, Mikushev V M and Charnaya E V 1992 *Sov. Phys.–Solid State* **34** 1753
[8]   Mavlonazarov I, Mikushev V M and Charnaya E V 1992 *JETP Lett.* **56** 13
[9]   Mavlonazarov I and Mikushev V M 1992 *Sov. Phys.–Solid State* **34** 2257
[10] Goldman M 1970 *Spin Temperature and Nuclear Magnetic Resonance in Solids* (Oxford: Clarendon)
[11] Antokol'skii G L, Charnaya E V and Shutilov V A 1973 *Sov. Phys.–Solid State* **15** 2167
[12] Kuleshov A A, Mikushev V M, Stolypko A L *et al* 1986 *Sov. Phys.–Solid State* **28** 1837
[13] Kuleshov A A, Stolypko A L, Charnaya E V and Shutilov V A 1987 *Sov. Phys.–Dokl.* **32** 308
[14] Szabo A 1962 *J. Chem. Phys.* **36** 562
[15] Simmons W W, O'Sullivan W J and Robinson W A 1962 *Phys. Rev.* **127** 1168
[16] Verber C M, Mahon H P and Tanttila W H 1962 *Phys. Rev.* **125** 1149
[17] Abragam A and Bleaney B 1970 *Electron Paramagnetic Resonance of Transition Ions* (Oxford: Clarendon)